RESEARCH ARTICLE OPEN ACCESS

‘Hybrid Vehicle Evolution and Future’

Rajkumar patil
Government College of Engineering And Research, Avasari, Mechanical Engineering , Savitribai Phule Pune University

Abstract:

These instructions give you guidelines for preparing papers for ‘Hybrid vehicle evolution and future’ in International Journal of Science Technology and Engineering. Use this document as a template if you are using Microsoft Word 6.0 or later. Otherwise, use this document as an instruction set. The electronic file of your paper will be formatted further at International Journal of Engineering and Technology. Define all symbols used in the abstract. Do not cite references in the abstract. Do not delete the blank line immediately above the abstract; it sets the footnote at the bottom of this column.

Keywords — **About four key words or phrases in alphabetical order, separated by commas.**

1.INTRODUCTION

A coupling is a device used to connect two shafts together at their ends for the purpose of transmitting power. Couplings do not normally allow disconnection of shafts during operation, however there are torquelimiting couplings which can slip or disconnect when some torque limit is exceeded.

The primary purpose of couplings is to join two pieces of rotating equipment while permitting some degree of misalignment or end movement or both. By careful selection, installation and maintenance of couplings, substantial savings can be made in reduced maintenance costs and downtime.

The Thomson constant velocity joint is a constant velocity joint with no parasitic bearing of sliding surfaces. This invention offers a revolution in the design of many transmission system, for instance in vehicular, marine, manufacturing, industrial and aeronautical application.

Thomson constant velocity joint is essentially two cardan joints assembled co-axially where the cruciform-equivalent members of each are connected to one another by trunions and bearings which are constrained to continuously lie on the homokinetic plane of the joint.

Basically the TCVJ has the same constructions as a normal cardan joint but does not suffer the dynamic loads due to fluctuating angular velocity of intermediate shaft and load, as is the case where cardan joints are used. As a result, the Thomson constant velocity joint has a life exceeding an ordinary cardan joint. There is no untried technology in the Thomson constant velocity joint. It is essentially identical to two cardon joints in its torque transmission. There are various constant velocity joint series available; constant, double constant velocity variable angle joints, for shaft angles to 30 degree. Even 90 degrees can be realized wit rigid and multiple rigid, angle constant velocity joint.

1.1 Problem Statement

In any direct mechanical drive system, there exists a need to couple the variety of driven elements that may be included. The majority of drive elements, including gear reducers, lead screws, and a host of other components, are driven by shafting that is supported by multiple bearings. This allows for shafting to be held extremely straight and rigid while rotating, avoiding any possible balancing and support problems. Because of this rigid support, it is virtually impossible to avoid slight misalignments between a driving and driven shaft when they are connected. Present technology in joints offers higher cost of joints, larger space and variable speed ratio if misalignment is present. The main concept is to lower cost of production, space requirement and simply technology of manufacture as compared to present CVJ in market.

1.2 Objectives

a) Design & drawing of kinematic linkage to deliver parallel as well angular offset over a range.
b) Development & manufacturing of drive.
c) Testing of drive to derive the performance.
d) Plot Performance Characteristic Curves.

1.3 Scope

The following features of the drive will lead to application of drive in variety of field applications:

a) **Step-less variation of angular offset:** Any displacement between 0 to 60 mm can be obtained .Hence the drive provides flexibility in operation and setting as prime mover location can be varies as per space available.
b) **Wide range of angular displacement:** The wide range of angular displacement 30 to 65 degrees enables to get vibration free power transmission at high speed. This will be especially useful in spring making machinery, textile machinery, printing machinery and automatic transfer lines.
c) **Compact size:** The size of the gear less variable speed reducer is very compact; which makes it low weight and occupies less space in any drive.
d) **Ease of operation:** The changing of angular and angular offset is gradual one hence no calculations of speed ratio required for change gearing .Merely by rotating hand wheel speed can be changed
e) **Singular control:** Entire range of offset is covered by a single hand wheel control.

1.4 Methodology

Following activities will be carried out during this dissertation work. It includes literature survey, system design, mechanical design, fabrication, assembly, testing and experimental analysis, and comparative study etc.

1.4.1 Literature review. Study of various power transmission drives in machine tool systems using various drive-train handbooks, United State Patent documents, Technical papers, etc.

1.4.2 Development of theory.

A) System Design:

This part includes the design and development for the kinematic linkage as per the geometry to produce the desired output

B) Mechanical Design:

This part includes the design and development of linkages, selection of suitable drive motor, strength analysis of various components under the given system of forces

1.4.3 Fabrication:

Suitable manufacturing methods will be employed to fabricate the components and then assemble the test set –up. The fabrication will be carried out as per layout shown below

1.4.4 Testing:

Testing of the joint to derive performance characteristics namely:

a) Torque vs. Speed.
b) Power vs. Speed.
c) Efficiency vs. Speed.
d) Maximum angular offset, and performance at maximum parallel offset.
e) Maximum angular offset and performance at maximum angular offset.

2 LITERATURE REVIEW

2.1 Ian Watson, B. Gangadhara Prusty and John Olsen have stated in research paper titled "Conceptual design optimization of a constant velocity coupling" that The Thompson Coupling operates using the robust double Cardan mechanism. Constant velocity and determinate linkage kinematics are maintained by a spherical pantograph. This mechanism forms an extra loop attached to the intermediate shaft in the double Cardan linkage, and consequently constrains this shaft to bisect the axis of input and output. Closed-form expressions for its motion and the rotation of the double Cardan joint are derived by consideration of spherical linkage kinematics. These expressions are then used to drive basic conceptual design optimization, whose goal is to reduce induced driveline vibration. The findings of this optimization are discussed with respect to the current design of the Thompson joint. Improvements in induced driveline vibration are possible, subject to the satisfaction of other coupling design criteria.

2.2 Chul-Hee Lee and Andreas A. Polycarpou has proposed in their research paper titled "A phenomenological friction model of tripod constant velocity (CV) joints" that constant velocity (CV) joints have been favored for automotive applications, compared to universal joints, due to their superiority of constant velocity torque transfer and plunging capability. High speed and sport utility vehicles with large joint articulation angles, demand lower plunging friction inside their CV joints to meet noise and vibration requirements, thus requiring a more thorough understanding of their internal friction characteristics. A phenomenological CV joint friction model was developed to model the friction behavior of tripod CV joints by using an instrumented CV joint friction apparatus with tripod-type joint assemblies. Experiments were conducted under different operating conditions of oscillatory speeds, CV joint articulation angles, lubrication, and torque. The experimental data and physical parameters were used to develop a physics-based phenomenological CV joint dynamic friction model. It was found that the proposed friction model captures the experimental data well, and the model was used to predict the external generated axial force, which is the main source of force that causes vehicle vibration problems.

2.3 Majid Yaghoubi, Seyed Saeid Mohtasebi, Ali Jafary and Hamid Khaleghi in their research worktitled "Design, manufacture and evaluation of a newand simple mechanism for transmission of powerbetween intersecting shafts up to 135 degrees(Persian Joint)" has introduced a new mechanismwhich is designed for the transmission of powerbetween two intersecting shafts. The mechanismconsists of one drive shaft and one driven shaft, sixguide arms, and three connecting arms. Theintersecting angle between the input shaft and theoutput shaft can be varied up to 135° while thevelocity ratio between the two shafts remainsconstant. The research also includes a kinematic **analysis** and a simulation using Visual NASTRAN,Autodesk Inventor Dynamic and COSMOS Motion.The software showed that this mechanism cantransmit constant velocity ratios at all angles betweentwo shafts. By comparing the graphs of analyticalanalysis and simulation analysis, validity of equations was proved.

2.4 Katsumi Watanabe and Takashi Matsuura in their research paper titled "Kinematic Analyses of Rzeppa Constant Velocity Joint by Means of Bilaterally Symmetrical Circular-Arc-Bar Joint" has proposed that mechanism whose elements are bilaterally symmetrical with respect to the bisecting plane of driving and driven rotational axes is able to use as the constant velocity joint. The constant velocity joint that is composed of input and output shafts, two circular-arc elements and the frame is a most elementary joint. The closed loop equation of the circular-arc-bar joint whose kinematic constants are any values is deduced in the form of the quadratic equation of the output angle. The Rzeppa constant velocity joint is composed of several sets of the ball and two circular-arc grooves. A relative motion of the ball to two circular-arc grooves is analyzed and the output angle error in a practical use which contains sinusoidal fluctuations with periods 2π, $2\pi/3$, and $2\pi/6$ is simulated by the circular-arc-bar constant velocity joint.

2.5 Tae-Wan Ku, Lee-Ho Kim and Beom-Soo Kang in their research work titled "Multi-stage coldforging and experimental investigation for the outerrace of constant velocity joints" has explored that asan important load-supporting automobile part thattransmits torque between the transmission and thedriven wheel, the outer race of CV (constant velocity)joints with six inner ball grooves has beenconventionally produced by the multi-stage warmforging processes, which involves several operationsincluding forward extrusion, upsetting, backwardextrusions, sizing and necking, as well as additionalmachining. There is still no choice but to produce thecomplex shaped components other than by this warmforging process. As an alternative, multi-stage coldforging process is presented to replace thesetraditional warm forging. The multi-stage coldforging procedure is first considered through aprocess assessment regarding the traditional multistagewarm forging one. Then, the process issimplified and redesigned as one operation toproduce the forged outer race and the backwardextrusions of the traditional process, and the sizingand necking are also combined into a single sizing neckingprocess.

2.6 Research Update:U-Joints versus Constant Velocity Joints (ISSN 1188-4770, Group 12 (h))

2.6.1 Cardan Joint

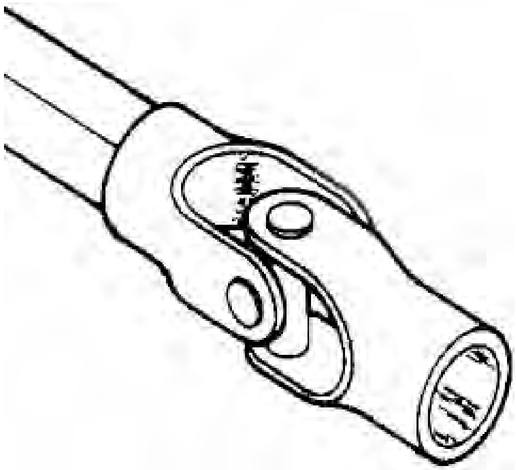

Fig 2.6.1: Typical cardan joint

Until fairly recently, Cardan joints were the only option available for agricultural applications, and are still very common today. A single Cardan joint consists of a pairof U-shaped yokes on the ends of the adjoining shafts joined through beatings to a metal cross. However, a single Cardan joint is limited to a 15° deviation from a straight line beforefluctuations in drive shaft speed and/or vibration begin to occur. The useful life of the Cardan joint can be drastically reduced because of vibration. They are usually used in pairs to increase the maximum operating range to 30° and to minimize speed fluctuations and vibration. With older square telescopic drive shafts, it was possible to connect the shaft so that the Cardan joints were out of phase (rotated 90° to each other). This could create a significant vibration problem. However, modern drive shafts are designed so that the telescopic shaft will only fit together by turning the sections in increments of 180°, ensuring the joints are always in phase.

It was also important that the vertical and horizontal angles of the two Cardan joints was equal to further reduce velocity fluctuation and associated driveline vibration. This could be accomplished by modifying the drawbar and machine hitch lengths so that the distances between the hitch point and the ends of the output and input shafts were equal. A more detailed explanation of PTO vibration can be found in the PAMI publication, Gleanings, 441. The life of a typical double Cardan joint drive shaft is reduced to 75% for 200 deviation from a straight line, and is halved when operating at a straight-line deviation of 30°.

2.6.2 Constant Velocity Joint

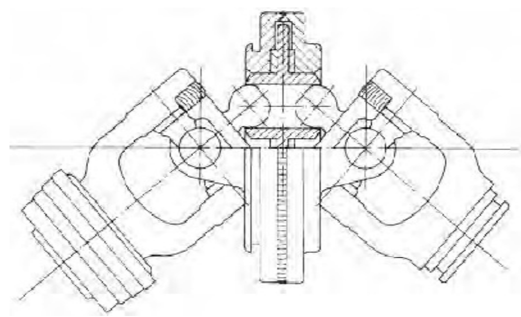

Fig 2.6.2: Typical CV Joint

The development of Constant Velocity (CV) joints has greatly improved the angle at which a driveline may operate from a straight line before loss of power and/or vibration occurs. The Constant Velocity joint's driving members are steel balls constrained in curved grooves between the forks of the joint. The design is such that a CV joint may operate efficiently up to a 80° deviation from a straight line. By operating in pairs, the angle can be increased accordingly. As with the Cardan joint, the effective life of a CV joint will be shortened as joint angles increase. While equalization of joint angles is still important, it is less of a concern for CV joints by their nature. For large angles, there still may be some vibration if the joint angles are not equal. Some new equipment designs require drivelines that have large joint angles. This is where wide-angle Constant Velocity joints shine. CV joints are necessary for high velocity power transmission and for axles and kingpins of steered traction wheels on modern farm machinery.

2.6.3 Cost Considerations

Constant Velocity Joints are more expensive than Cardan joints. But replacing Cardan joints over time may in fact, become more expensive than an investment in the more versatile CV joint. CV joints are necessary where high velocity power transmission is required and operating angles are acute. Paired Cardanjoints are not able to transmit power properly where angles exceed 30° without losing power and/or causing vibrations. Cardan joints pressed into operation where they are unsuitable results in dramatically reduced life of the joint.

2.6.4 The Constant Velocity Mystery

Constant velocity in PTO drivelines is an ideal operating condition, and can be achieved with both Cardan joints and constant velocity joints. But there is more than one method of achieving constant velocity in drivelines. A typical driveline with Cardan joints at each shaft end will have constant velocity if the operating geometry is arranged so: that the yokes on the intermediate shaft are in phase and the hitch point is centred between the PTO output shaft on the tractor and the PTO input shaft on the implement. Another method of achieving contant velocity is through the use of Double Cardan joints, which overcome the limitations of PTO drivelines that have two or more sets of single Cardan joints. Double Cardan joints are typically used where operating angles are too large for single cardan joints. A Double Cardan joint is essentially two single Cardan joints connected by a coupling yoke that contains a centering mechanism. This centering mechanism keeps the input and output shafts in the same plane, regardless of the operating angle. A Wide-angle Double Cardan joint uses a centering mechanism comprised of a flat disc withsockets that support the ball stud yokes. This centering mechanism compensates for velocity fluctuations of the two Cardan joints, thereby providing a constant velocity output. Other Double Cardan joints use centering mechanisms that incorporate a ball and stud mechanism, or a ball and seat mechanism. Double Cardan joints with these centering mechanisms are considered to be near constant velocity joints because their centering mechanisms do not split the misalignment between the shafts equally for all operating angles. Consequently, these joints do not produce true constant velocity output - except at the design angle. (All joints are designed to transfer power efficiently up to a maximum angle - the design angle. Operation beyond the design angle results in excessive vibration.) For practical purposes, the resulting velocity fluctuation is negligible. In comparison, the centering mechanism in a Wide-angle Double Cardan joint always splits the misalignment between shafts equally. As a result, the wide-angle Double Cardan joint has a true constant velocity output at all operating angles up to the design angle. Double Cardan joints with ball-and-stud or ball-and-seat mechanisms are typically designed for higher speeds than are Wide-angle Double Cardan joints. The Wide-angle Double Cardan joint is most commonly used where speeds do not exceed 1000 rpm.

3 SYSTEM DESIGN

3.1 Design Considerations

In system design we mainly concentrated on the following parameters: -

3.1.1 System Selection Based on Physical Constraints

While selecting any machine it must be checked whether it is going to be used in a large-scale industry or a small-scale industry. In our case it is to be used by a small-scale industry. So space is a major constrain. The system is to be very compact so that it can be adjusted to corner of a room. The mechanical design has direct norms with the system design. Hence the foremost job is to control the physical parameters, so that the distinctions obtained after mechanical design can be well fitted into that.

3.1.2 Arrangement of Various Components

Keeping into view the space restrictions the components should be laid such that their easy removal or servicing is possible. More over every component should be easily seen none should be hidden. Every possible space is utilized in component arrangements.

3.1.3Components of System

As already stated the system should be compact enough so that it can be accommodated at a corner of a room. All the moving parts should be well closed & compact. A compact system design gives a high weighted structure which is desired.

3.1.4 Man Machine Interaction

The friendliness of a machine with the operator that is operating is an important criteria of design. It is the application of anatomical & psychological principles to solve problems arising from Man – Machine relationship.

3.1.5 Chances of Failure

The losses incurred by owner in case of any failure is an important criteria of design. Factor safety while doing mechanical design is kept high so that there are less chances of failure. Moreover periodic maintenance is required to keep unit healthy.

3.1.6 Servicing Facility

The layout of components should be such that easy servicing is possible. Especially those components which require frequents servicing can be easily disassembled.

3.1.7 Height of Machine from Ground

For ease and comfort of operator the height of machine should be properly decided so that he may not get tired during operation. The machine should be slightly higher than the waist level, also enough clearance should be provided from the ground for cleaning purpose.

3.1.8 Weight of Machine

The total weight depends upon the selection of material components as well as the dimension of components. A higher weighted machine is difficult in transportation & in case of major breakdown, it is difficult to take it to workshop because of more weight.

3.2 Selection of Motor

The metric system uses kilowatts (kW) for driver ratings. Converting kW to torque:

T= kWx84518 rpm

Where

T = the torque in inch pounds

kW the motor or other kilowatts

rpm= the operating speed in revolutions per minute

84518 = a constant used when torque is in inch-pounds. Use 7043 for foot-pounds, and 9550 for Newton-meters

0.3 = kW x 9550 /1200

kW = 0.038 kW

Thus the minimum input power required will be 38 watt.

3.2.1 Drive Motor

Type: - Single Phase Ac Motor.

Power: - 1 /15 Hp. (50 Watts)

Voltage: - 230 Volts, 50 Hz

Current: - 0.5 Amps

Speed: - Min = 0 rpm ,Max = 9500 rpm

TEFC Construction, Commentator Motor.

3.3 Design of Belt Drive

Power is transmitted from the motor shaft to the input shaft of drive by means of an open belt drive,

Motor pulley diameter = 20 mm

Input shaft pulley diameter = 100 mm

Reduction ratio = 5

Input shaft speed = 9500/5 = 1900 rpm

T motor = 0.05 Nm

Torque at Input shaft = 5 x 0.05 = 0.25 Nm

3.3.1 Design of Open Belt Drive

Motor pulley diameter = 20 mm

Input shaft pulley diameter = 110 mm

Reduction ratio = 5

Coefficient of friction = 0.23

Maximum allowable tension in belt = 200 N

Center distance = 120

Wrap angle of pulley

$\alpha = 180 - 2\sin^{-1}[(D-d)/2C]$

$\alpha = 180 - 2\sin^{-1}[(110-20)/(2x120)]$

$\alpha = 136^0$

$\alpha = 2.37^c$

Now,

$e^{\mu\alpha/\sin(\theta/2)} = e^{0.2 \text{ x } 2.37\sin(40/2)} = 4$

Width (b_2) at base is given by

$b_2 = 6\text{-}2(4 \tan 20) = 3.1$

Area of cross section of belt = ½{6 + 3.1}x 4

A = 18.2 mm2

Now mass of belt /m length = 0.23 kg/m

V = ΠDN/ (60 x 1000) = 4.188m/sec

$Tc = m V^2$

Tc = 4.034 N

T_1 = Maximum tension in belt – Tc

T_1= 195.966 = 196 N

$T_1 / T_2 = e^{\mu\alpha/\sin(\theta/2)} = 4$

T_2 = 49 N

3.3.2 Result

Tension in tight side of belt (T_1) = 196 N

Tension in slack side of belt (T_2) = 49 N

3.4 Design of Input Shaft

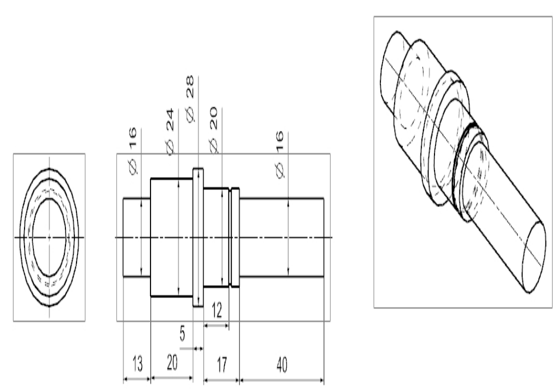

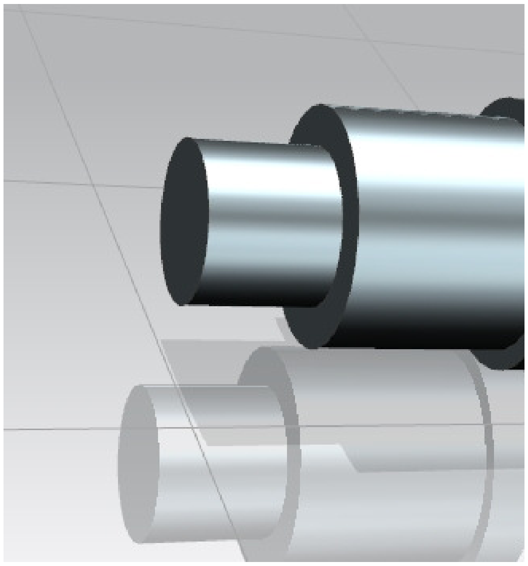

Fig3.4.: Design of input shaft.

3.4.1Material Selection: -Ref: - Psg (1.10 & 1.12) + (1.17)

Designation	Ultimate Tensile Strength N/r
EN 24	800

Table 3.4.1: material selection of input shaft

fs_{max} = UTS/FOS = 800/2 = 400 N/mm^2

This is the allowable value of shear stress that can be induced in the shaft material for safe operation.

Check for torsional shear failure of shaft.

$$Te = \frac{\Pi\, fs\, d^3}{16}$$

$$fs_{act} = \frac{16 \times 0.25 \times 10^3}{\Pi \times 16^3}$$

$fb_{act} = 0.310\ N/mm^2$

As; $fs_{act} < fs_{all}$

Input is safe under torsional load.

3.4.1 Ansys Model

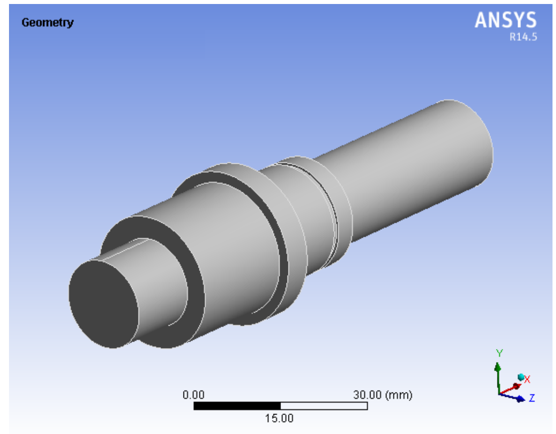

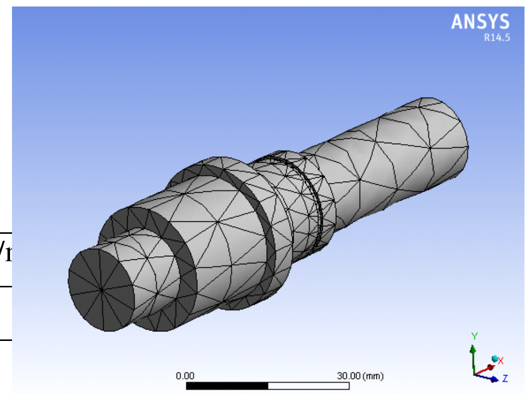

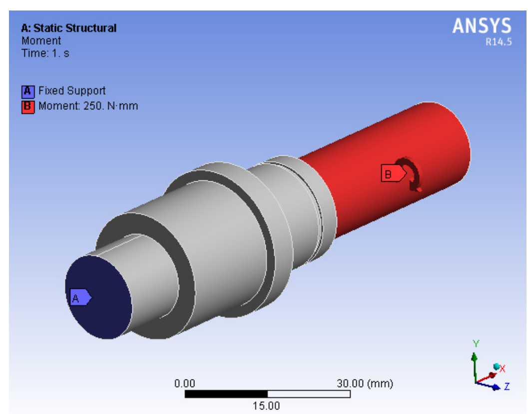

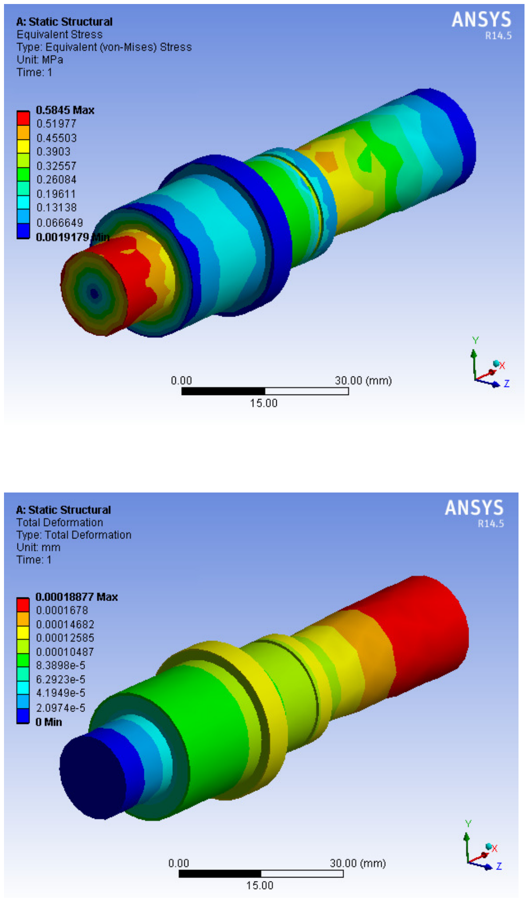

Fig 3.4.1: Ansys model of input shaft

3.4.2Result & discussion

Part Name	Maximum theoretical stress N/mm^2	Von-mises stress N/mm^2	Total deformation mm	Result
Input Shaft	0.310	0.5845	0.0001887	safe

Table 3.4.2: Result table for input shaft

3.4.3Conclusion.

a) Maximum stress by theoretical method and Von-mises stress are well below the allowable limit, hence the input shaft is safe.

b) Shaft shows negligible deformation.

3.5Design of Input Coupler Body

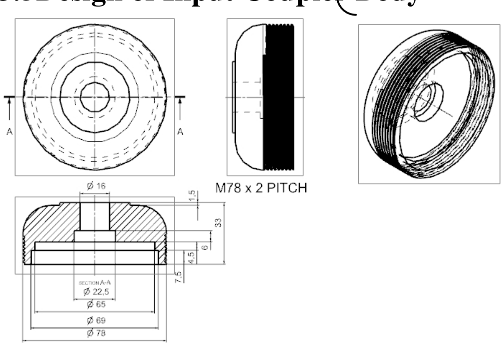

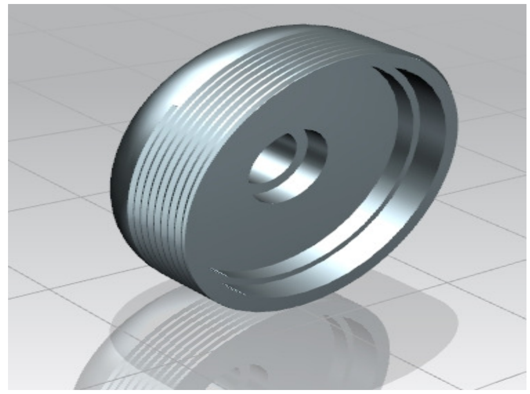

Fig 3.5: Design of input coupler body

3.5.1Material Selection.

Designation	Ultimate Tensile strength N/mm^2
Aluminium	400

Table 3.5.1:Material selection of input coupler body

fs_{max} = UTS/FOS =400/2 = $200 N/mm^2$

Check for torsional shear failure:-

$$T = \frac{\Pi \times fs_{act} \times (Do^4 - Di^4)}{16Do}$$

$$0.25 \times 10^3 = \frac{\Pi \times fs_{act}}{16} \times \frac{22.5^4 - 16^4}{22.5}$$

$fs_{act} = 0.15 N/mm^2$

As; $fs_{act} < fs_{all}$

Input coupler body is safe under torsional load.

3.5.2 Ansys Model

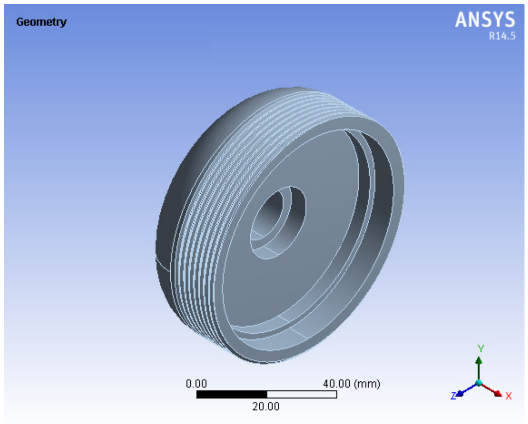

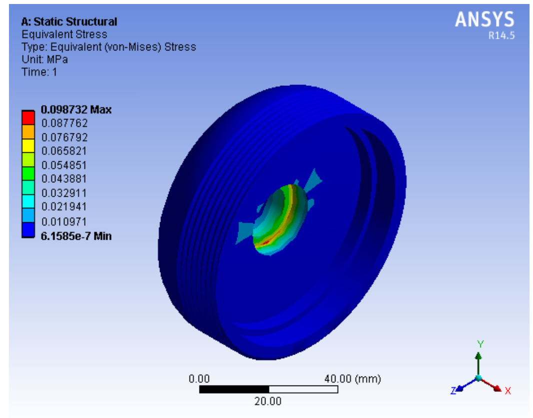

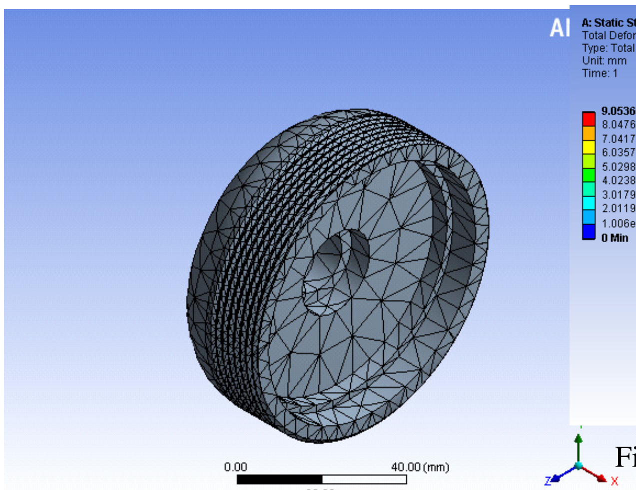

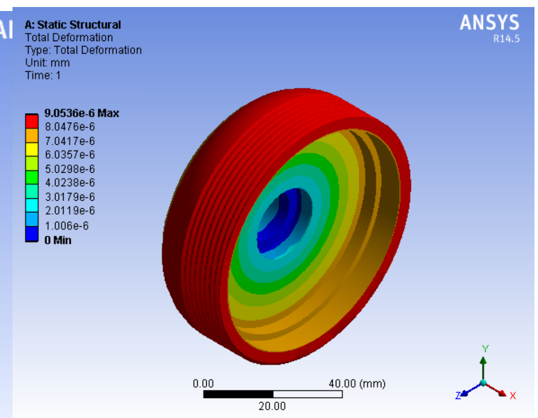

Fig 3.5.2: Ansys model of input coupler body

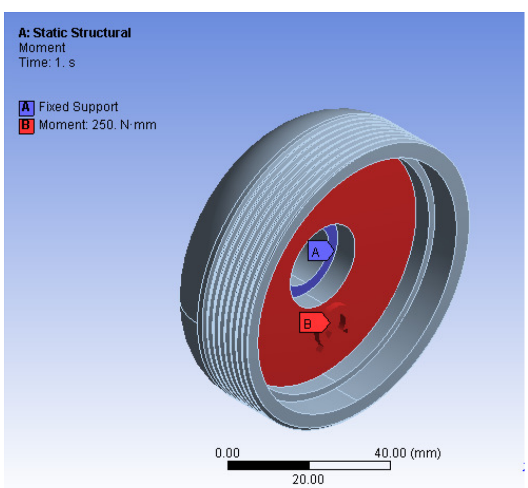

3.5.3Result & Discussion

Part Name	Maximum theoretical stress N/mm^2	Von-mises stress N/mm^2	Total deformation mm	Result
Input Coupler Body	0.15	0.098	9.06E-6	safe

Table 3.5.3:Result table for input coupler body

3.5.4Conclusion.

a) Maximum stress by theoretical method and Von-mises stress are well below the allowable limit, hence the input coupler body is safe.
b) Input coupler body shows negligible deformation.

3.6 Design of Input Coupler Ring

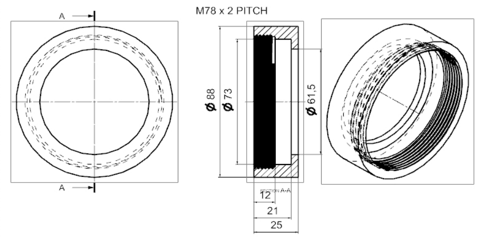

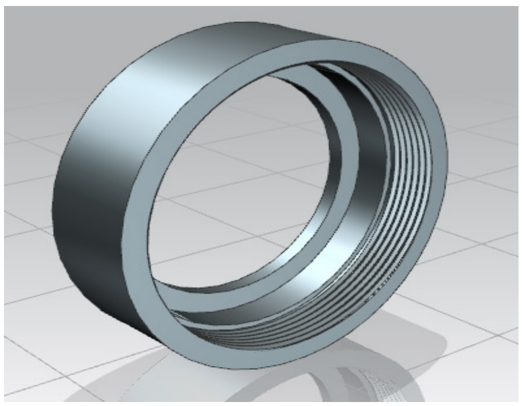

Fig 3.6:Design of input coupler ring

3.6.1 Material selection.

Designation	Ultimate Tensile strength N/mm^2	Yield strength N/mm^2
EN 24	800	680

Table 3.6.1: material selection for input coupler ring

$fs_{max} = 400 N/mm^2$

Check for torsional shear failure:-

$$T = \frac{\Pi}{16} \times fs_{act} \times \left(\frac{Do^4 - Di^4}{Do} \right)$$

$$0.25 \times 10^3 = \frac{\Pi}{16} \times fs_{act} \times \left(\frac{88^4 - 73^4}{88} \right)$$

$fs_{act} = 0.0035/mm^2$

As; $fs_{act} < fs_{all}$

Input Coupler ring is safe under torsional load

3.6.2Ansys Model

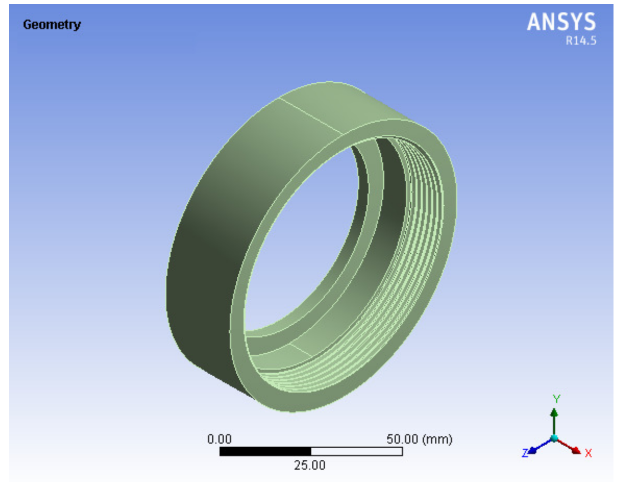

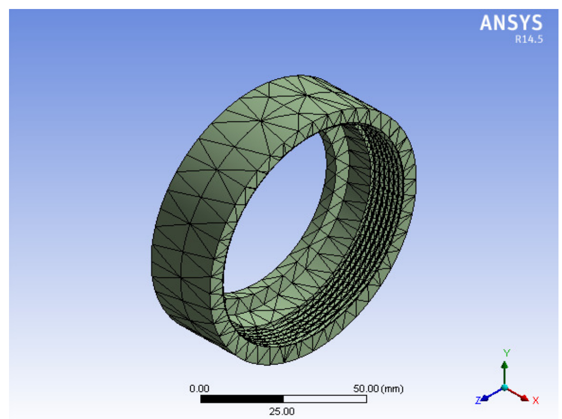

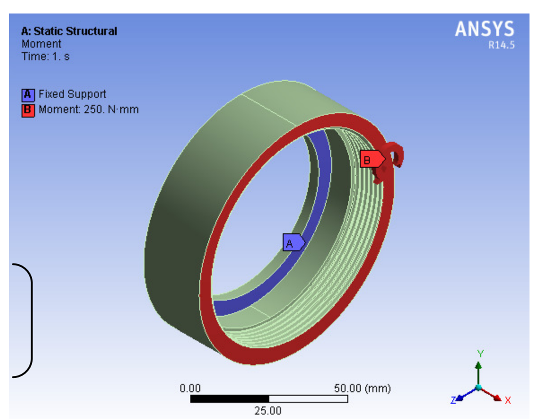

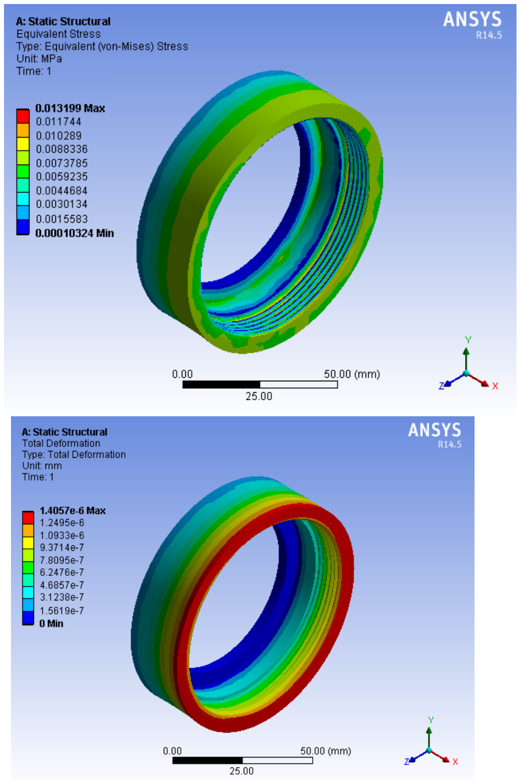

Fig 3.6.2: Ansys model of input coupler ring

3.6.3 Result & discussion

Part Name	Maximum theoretical stress N/mm^2	Von-mises stress N/mm^2	Total deformation mm	Result
Input Coupler Ring	0.0035	0.013	1.045E-6	safe

Table 3.6.3: Result table for input coupler ring

3.6.4 Conclusion.

a) Maximum stress by theoretical method and Von-mises stress are well below the allowable limit, hence the input coupler ring is safe.

b) Input coupler ring shows negligible deformation.**3.7Selection of Ball Bearing for Input Shaft**

Selection of bearing 6004 ZZ

The input shaft is held in two ball bearings that equally share the radial load on the shaft. Selecting; Single Row deep groove ball bearing as follows.

Series 60

IsI No	Bearing of basic design No (SKF)	D	D1	D	D_2	B	Basic capacity	
2AC04	6004	20	23	42	36	12	4500	7350

Table 3.7.1: Bearingdata (6004)

$P = X F_r + Y F_a$

Neglecting self-weight of carrier and gear assembly

For our application F_a=0

$P = X F_r$

Where F_r =Pt = T1+T2 = 196 +49 =245 N

Max radial load = F_r =245 N.

P= 145 N

Calculation dynamic load capacity of bearing.

$L = (C / P)^{p}$, where p= 3 for ball bearings.

For m/c used for eight hr of service per day;

L_H = 4000- 8000hr

But; $L= 60\ n\ L_H/10^6$

$L = 60 \times 1900 \times 4000 / 10^{6}$ mrev ....here speed of shaft is considered to be 1900 rpm

$L = 456$

Now; $456 = \frac{(C)^{3}}{(145)^{3}}$

$C = 1885N$

As the required dynamic capacity of bearing is less than the rated dynamic capacity of bearing;

Bearing is safe.

3.8 Design of Input Coupler Female Liner

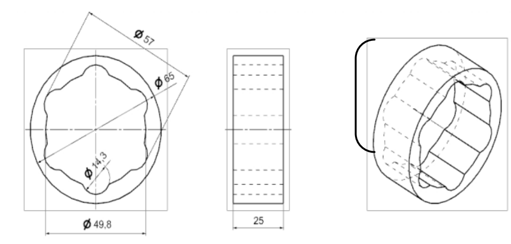

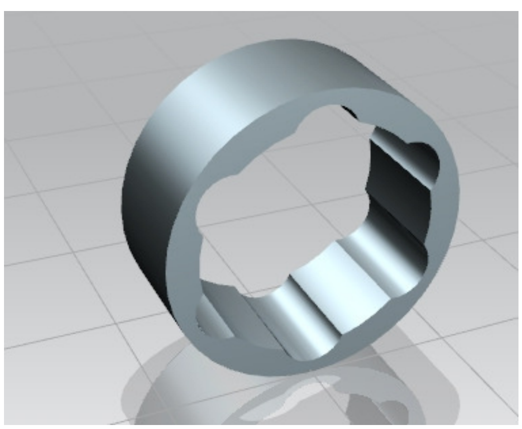

Fig 3.8: design of input coupler female liner

3.8.1 Material Selection

Designation	Ultimate Tensile strength N/mm^2	Yield strength N/mm^2
EN 24	800	680

Table 3.8.1: Material selection of input coupler female liner

$fs_{max} = 400N/mm^2$

Check for torsional shear failure:-

$$T = \frac{\Pi}{16} \times fs_{act} \times \left[\frac{Do^{4} - Di^{4}}{Do}\right]$$

$$0.25 \times 10^{3} = \frac{\Pi}{16} \times fs_{act} \times \left[\frac{65^{4} - 57^{4}}{65}\right]$$

$fs_{act} = 0.0113N/mm^2$

As; $fs_{act} < fs_{all}$

Input Coupler female liner is safe under torsional load.

3.8.2 Ansys Model

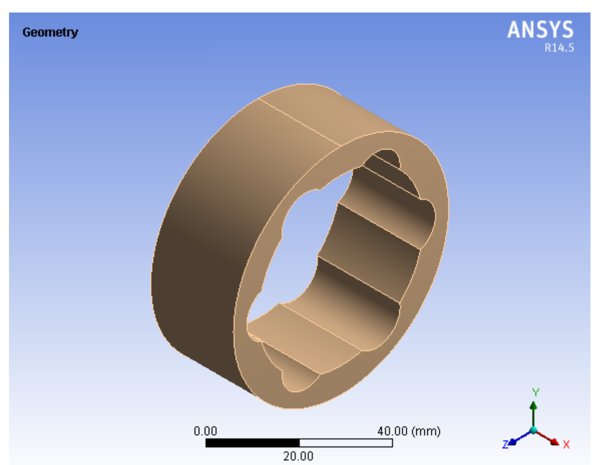

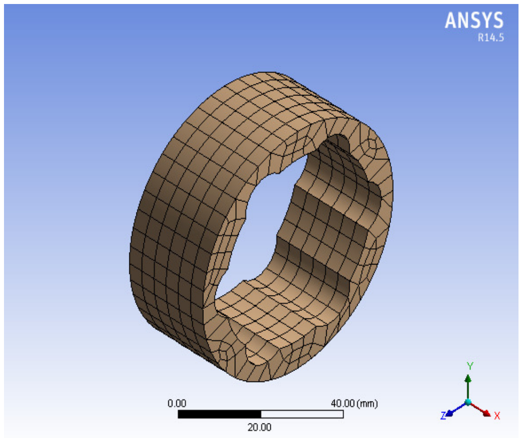

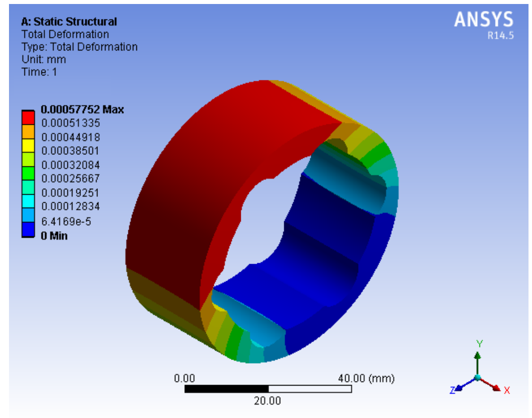

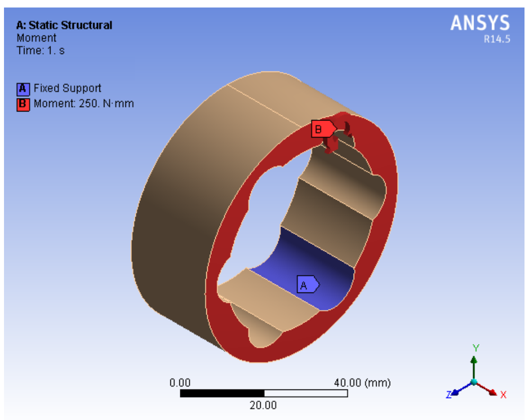

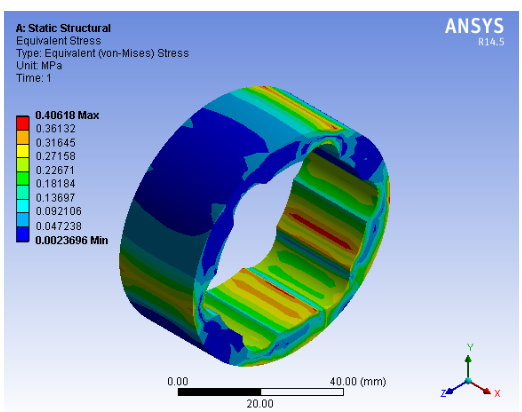

Fig 3.8.2: Ansys model of input coupler female liner

3.8.3 Result & Discussion

Part Name	Maximum theoretical stress N/mm^2	Von-mises stress N/mm^2	Total deformation mm	Result
Input coupler female liner	0.0113	0.40	1.045E-6	Safe

Table3.8.3: Result table for input coupler female liner

3.8.4 Conclusion

a) Maximum stress by theoretical method and Von-mises stress are well below the allowable limit, hence the input coupler ring is safe.

b) Input coupler ring shows negligible deformation

3.9 Design of Coupler Pin

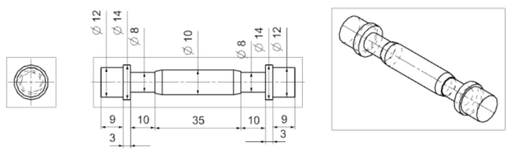

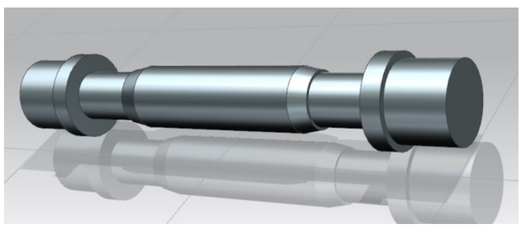

Fig 3.9: Design of coupler pin

3.9.1Material Selection: -Ref: - PSG (1.10 & 1.12) + (1.17)

Designation	Ultimate Tensile strength N/mm^2	Yield strength N/mm^2
EN 24	800	680

Table 3.9.1: Material selection of coupler pin

fs_{max} = uts/fos = 800/2 = 400 N/mm^2

This is the allowable value of shear stress that can be induced in the shaft material for safe operation.

Check for torsional shear failure of shaft

$$Te = \frac{\Pi}{16} fs\, d^3$$

$$fs_{act} = \frac{16 \times 0.25 \times 10^3}{\Pi \times 8^3}$$

fb_{act} = 2.4860 N/mm^2

As; $fs_{act} < fs_{all}$

Coupler pin is safe under torsional load.

3.9.2Ansys Model

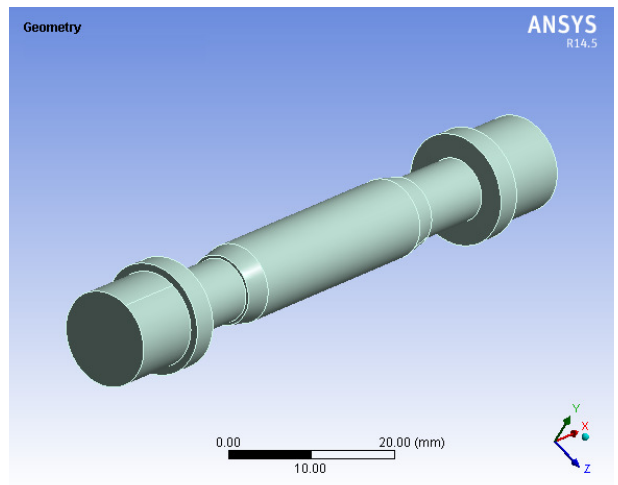

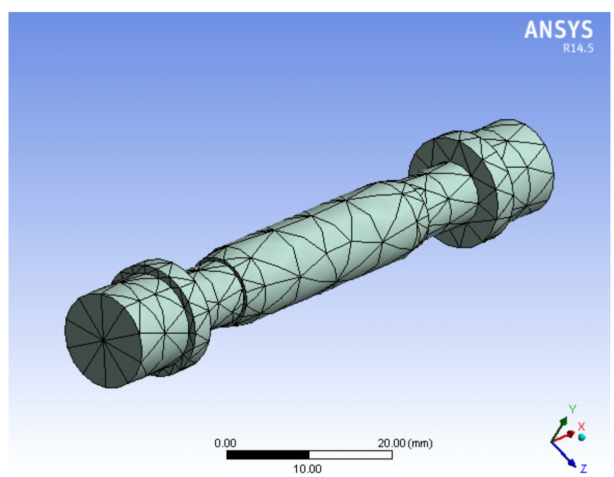

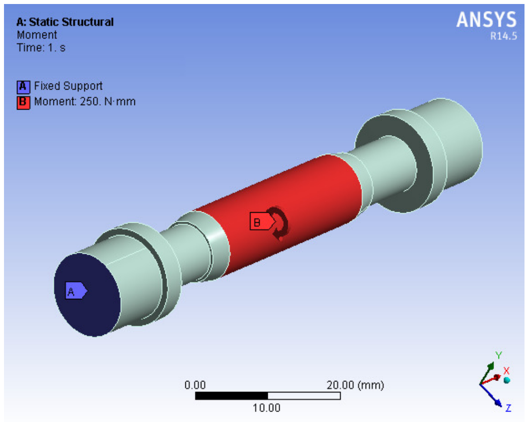

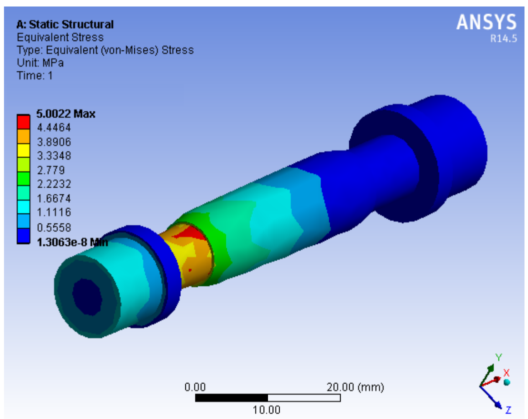

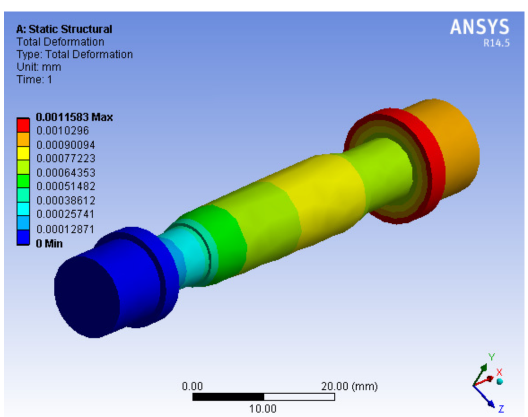

Fig 3.9.2: Ansys model of coupler pin

3.9.3 Results & Discussion

Part Name	Maximum theoretical stress N/mm^2	Von-mises stress N/mm^2	Total deformation mm	Result
Coupler pin	2.486	5.02	0.0011	Safe

Table 3.9.3: Result table for coupler pin

3.9.4 Conclusion

a) Maximum stress by theoretical method and Von-mises stress are well below the allowable limit, hence the coupler pin is safe.

b) Coupler pin shows negligible deformation.

3.10Design of Output Shaft

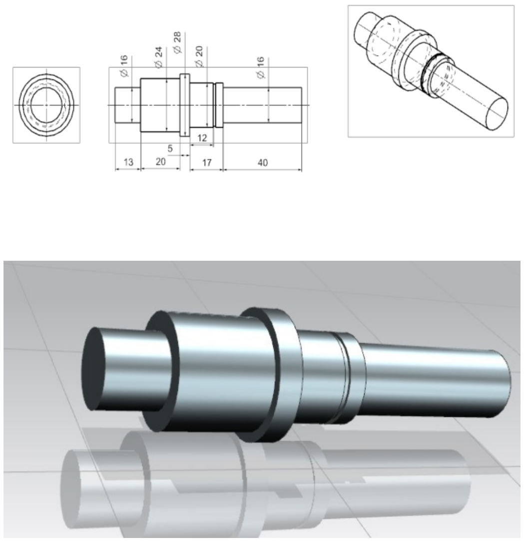

Fig 3.10: Design of output shaft

3.10.1Material selection

Designation	Ultimate TensileStrengthN/Mm^2	Yield Strength
EN 24	800	680

Table: 3.10.1: Material selection for output shaft

fs_{max} = UTS/FOS = 800/2 = 400 N/mm^2

This is the allowable value of shear stress that can be induced in the shaft material for safe operation.

Check for torsional shear failure of shaft

$$Te = \frac{\Pi}{16} fs\, d^3$$

$$fs_{act} = \frac{16 \times 0.25 \times 10^3}{\Pi \times 16^3}$$

fb_{act}= 0.310 N/mm^2

As; $fs_{act} < fs_{all}$

Output is safe under torsional load.

3.10.2 Ansys Model

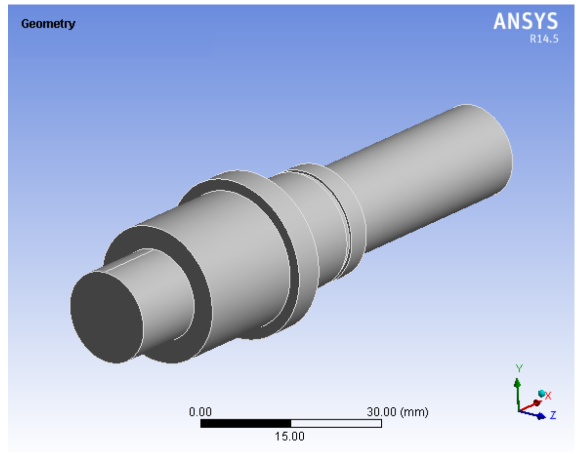

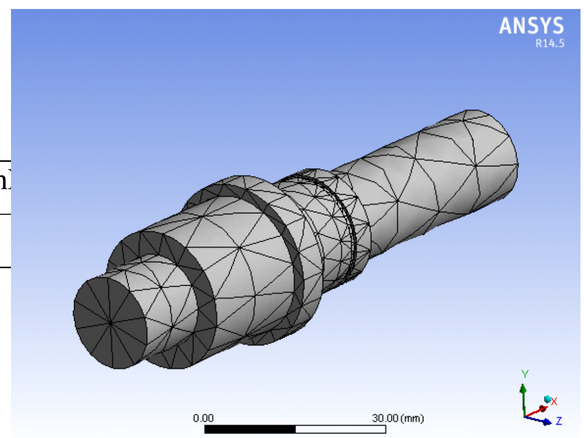

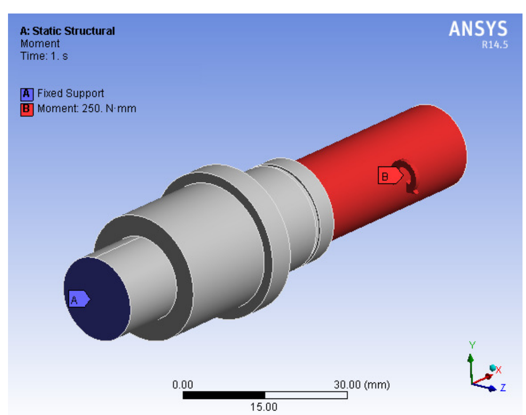

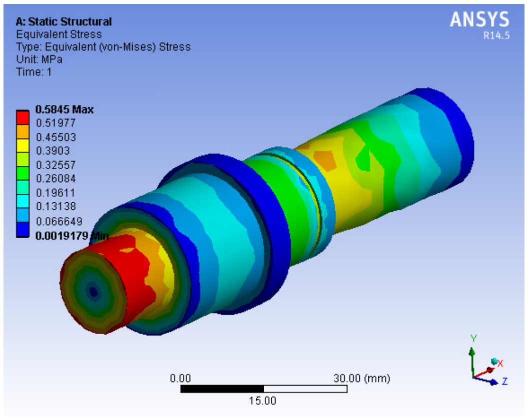

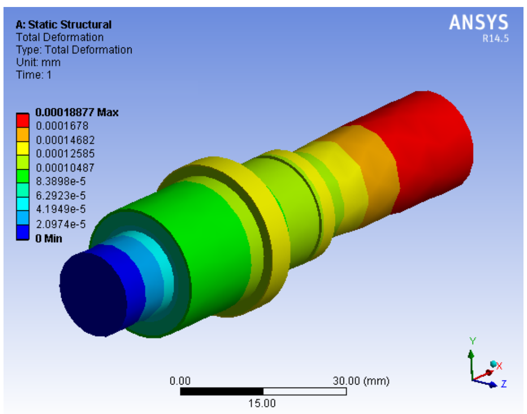

Fig 3.10.2: Ansys model of output shaft

3.10.3Result & Discussion

Part Name	Maximum theoretical stress N/mm^2	Von-mises stress N/mm^2	Total deformation Mm	Result
Output Shaft	0.310	0.5845	0.0001887	Safe

Table3.10.2: Result table for output shaft

3.10.4Conclusion.

a) Maximum stress by theoretical method and Von-mises stress are well below the allowable limit, hence the output shaft is safe.

b) Output Shaft shows negligible deformation.

3.11Design of Output Coupler Body

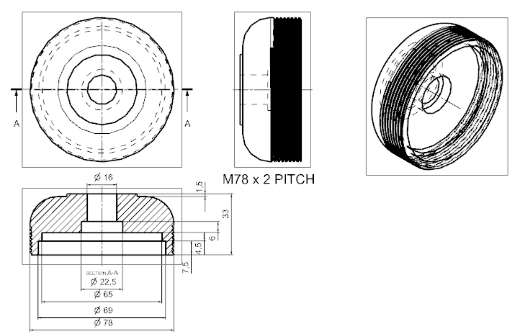

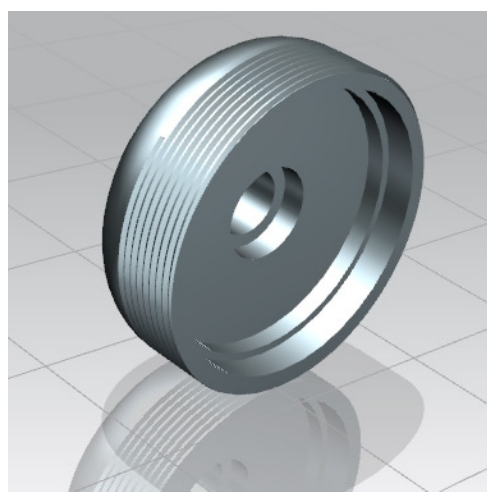

Fig 3.11: Design of output coupler body

3.11.1Material selection.

Designation	Ultimate Tensile strengthN/mm^2	Yield strength N/mm^2
Aluminum	400	280

Table3.11.1: Material selection for output coupler body

fs_{max} = UTS/FOS =400/2 = $200 N/mm^2$

Check for torsional shear failure:-

$$T = \frac{\Pi \times fs_{act} \times Do^4 - Di^4}{16 \quad Do}$$

$$0.25 \times 10^3 = \frac{\Pi \times fs_{act} \times 22.5^4 - 16^4}{16 \quad 22.5}$$

$fs_{act} = 0.15 N/mm^2$

As; $fs_{act} < fs_{all}$

Output coupler body is safe under torsional load.

3.11.2 Ansys Model

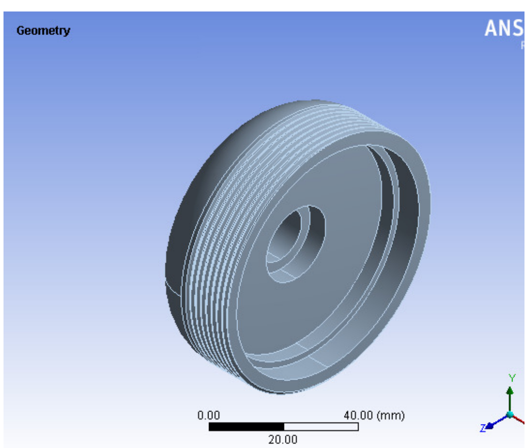

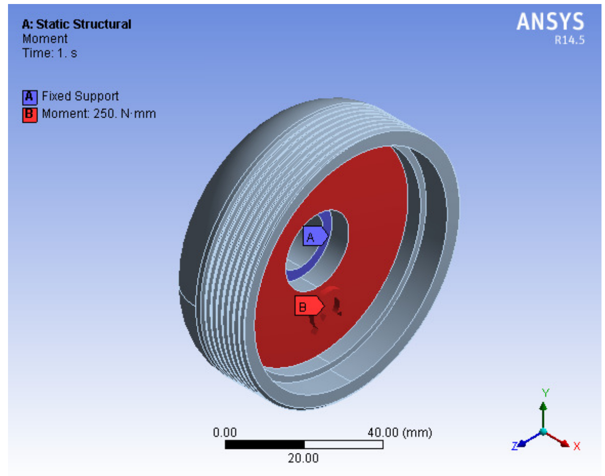

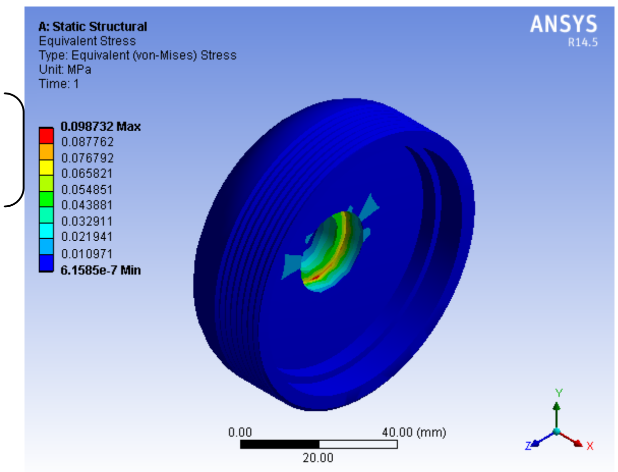

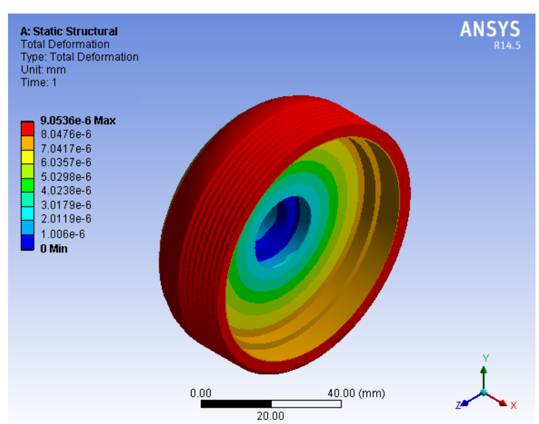

Fig 3.11.2: Ansys model of output coupler body

3.11.3Result & Discussion

Part Name	Maximum theoretical stress N/mm^2	Von-mises stress N/mm^2	Total deformation mm	Result
Output Coupler Body	0.15	0.098	9.06E-6	safe

Table 3.11.3: Result table for output coupler body

3.11.4Conclusion.

a) Maximum stress by theoretical method and Von-mises stress are well below the allowable limit, hence the output coupler body is safe.

b) Output coupler body shows negligible deformation.

3.12Design of Output Coupler Ring

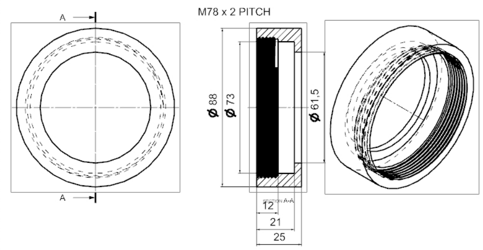

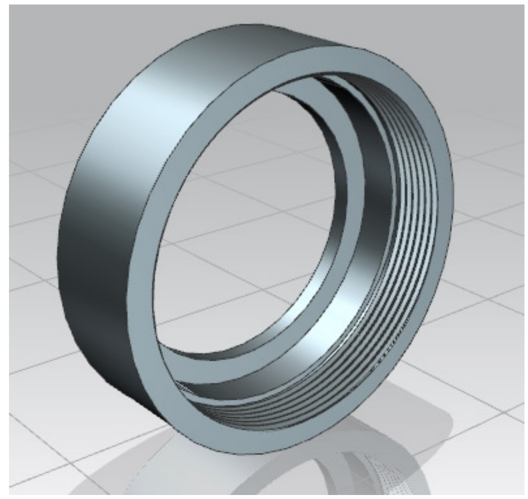

Fig 3.12: Design of output coupler ring

3.12.1Material selection.

Designation	Ultimate Tensile strength N/mm^2	Yield strength N/mm^2
EN 24	800	680

Table 3.12.1: Material selection for output coupler ring

$fs_{max} = 400 N/mm^2$

Check for torsional shear failure:-

$$T = \frac{\Pi \times fs_{act} \times (Do^4 - Di^4)}{16Do}$$

$$0.25 \times 10^3 = \frac{\Pi \times fs_{act} \times 88^4 - 73^4}{1688}$$

$fs_{act} = 0.0035\ N/mm^2$

As; $fs_{act} < fs_{all}$

Output coupler ring is safe under torsional load.

3.12.2 Ansys Model

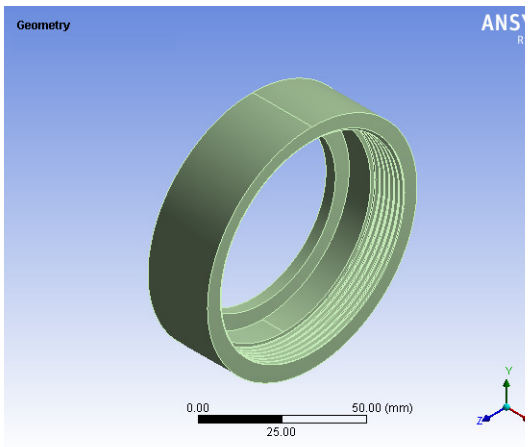

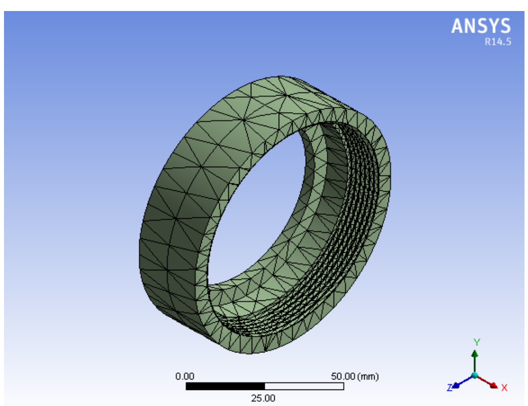

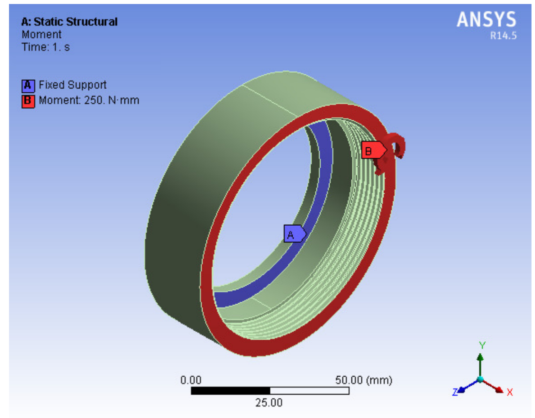

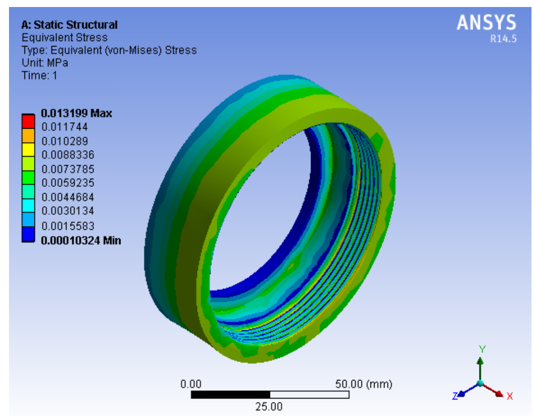

Fig 3.12.2: Ansys model of output coupler ring

3.12.3Result & Discussion

Part Name	Maximum theoretical stress N/mm^2	Von-mises stress N/mm^2	Total deformation mm	Result

Output Coupler Ring	0.0035	0.013	1.045E-6	Safe

Table 3.12.3: Result table for output coupler ring

3.12.4Conclusion.

a) Maximum stress by theoretical method and Von-mises stress are well below the allowable limit, hence the output coupler ring is safe.

b) Output coupler ring shows negligible deformation.

3.13Selection of Ball Bearing for Output Shaft

Selection of Bearing 6004 ZZ

The input shaft is held in two ball bearings that equally share the radial load on the shaft.

Selecting; Single Row deep groove ball bearing as follows.

Series 60

Sr No	Bearing of basic design No (SKF)	d	D1	D	D2	B	Basic capacity	
2AC04	6004	20	23	42	36	12	4500	7350

Table3.13.1: Bearing data (6004ZZ)

$P = X F_r + Y F_a$

Neglecting self-weight of carrier and gear assembly

For our application $F_a = 0$

$P = X F_r$

Where F_r =Pt = T1+T2 = 196 +49 =245 N

Max radial load = F_r =245 N.

P= 145 N

Calculation dynamic load capacity of bearing.

$L = (C / P)^p$, where p= 3 for ball bearings

For m/c used for eight hr of service per day;

L_H = 4000- 8000hr

But; $L = \frac{60\, n\, L_H}{10^6}$

$L = 60 \times 1900 \times 4000 / 10^6$ mrev ....here speed of shaft is considered to be 1900 rpm

$L = 456$

Now; $456 = \frac{(C)^3}{(145)^3}$

$C = 1885N$

As the required dynamic capacity of bearing is less than the rated dynamic capacity of bearing;

Bearing is safe.

3.14 Design of Output Coupler Female Liner

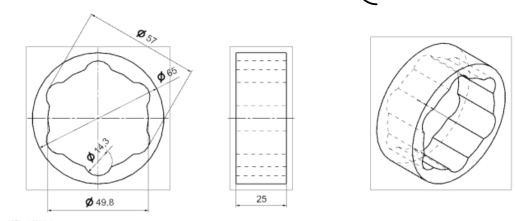

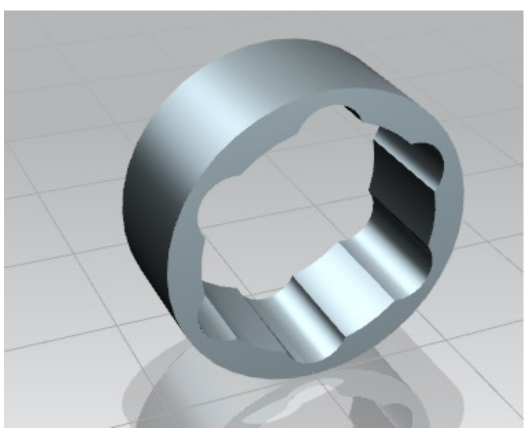

Fig 3.14: Design of output coupler female liner

3.14.1 Material selection.

Designation	Ultimate Tensile strength N/mm^2	Yield strength N/mm^2
EN 24	800	680

Table 3.14.1: Material selection for output coupler female liner

$fs_{max} = 400N/mm^2$

Check for torsional shear failure:-

$$T = \frac{\Pi \times fs_{act}}{16} \times \left(\frac{Do^4 - Di^4}{Do}\right)$$

$$0.25 \times 10^3 = \frac{\Pi \times fs_{act}}{16} \times \left(\frac{65^4 - 57^4}{65}\right)$$

$fs_{act} = 0.0113N/mm^2$

As; $fs_{act} < fs_{all}$

Output Coupler female liner is safe under torsional load.

3.14.2 Ansys model

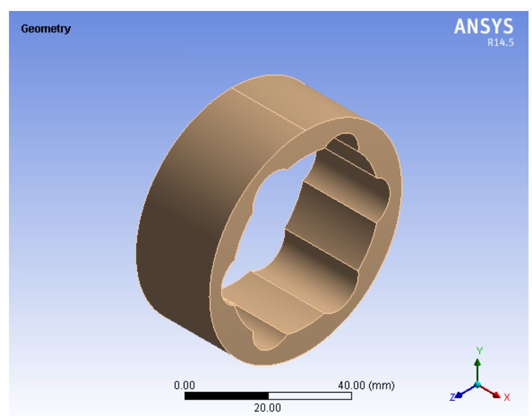

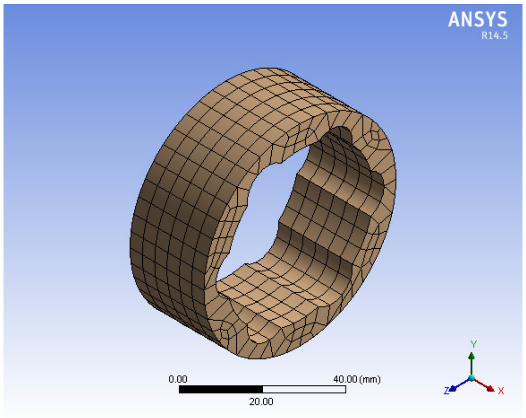

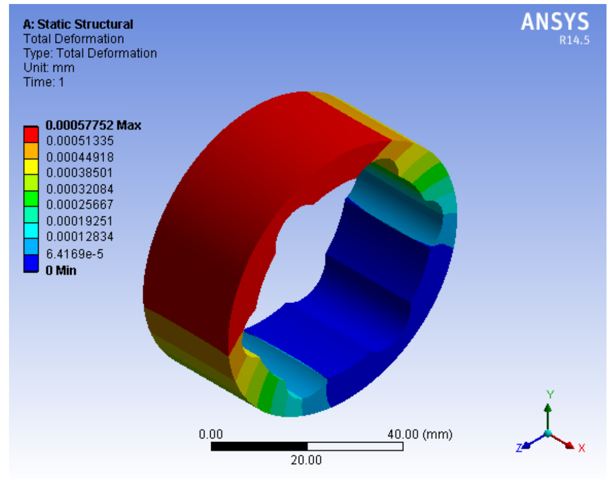

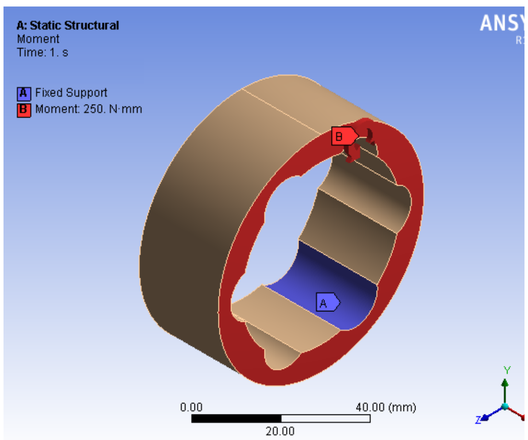

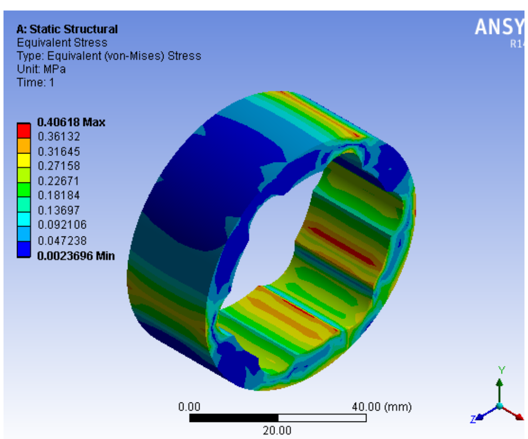

Fig 3.14.2: Ansys model of output coupler female liner

3.14.3 Result & Discussion

Part Name	Maximum theoretical stress N/mm^2	Von-mises stress N/mm^2	Total deformation mm	Result
Output coupler female liner	0.0113	0.40	1.045E-6	Safe

Table3.14.3: Result table for output coupler female liner

3.14.4 Conclusion

a) Maximum stress by theoretical method and Von-mises stress are well below the allowable limit, hence the output coupler female liner is safe.

b) Output coupler female linershows negligible deformation.**.15 Design of Trunion Holder**

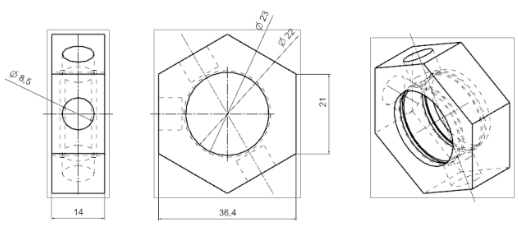

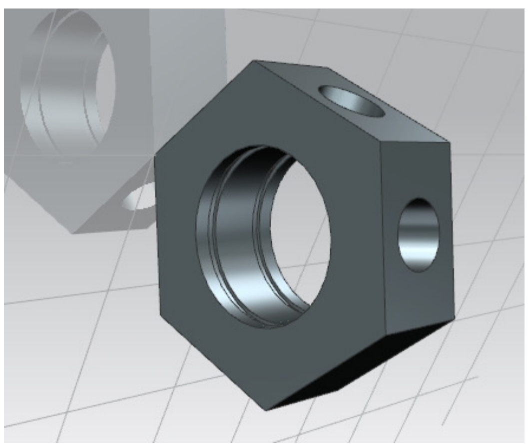

Fig 3.15: Design of trunion holder

3.15.1 Material selection.

Designation	Ultimate Tensile strength N/mm^2	Yield strength N/mm^2
Aluminium	400	280

Table 3.15.1: Material selection for trunion holder

fs_{max} = UTS/FOS =400/2 = $200 N/mm^2$

Check for torsional shear failure:-

$$T = \frac{\Pi}{16} \times fs_{act} \times \left(\frac{Do^4 - Di^4}{Do} \right)$$

$$0.25 \times 10^3 = \frac{\Pi}{16} \times fs_{act} \times \left(\frac{36.4^4 - 23^4}{36.4} \right)$$

fs_{act} = $0.2 N/mm^2$

As; $fs_{act} < fs_{all}$

Trunion holder is safe under torsional load.

3.15.2 Ansys Model

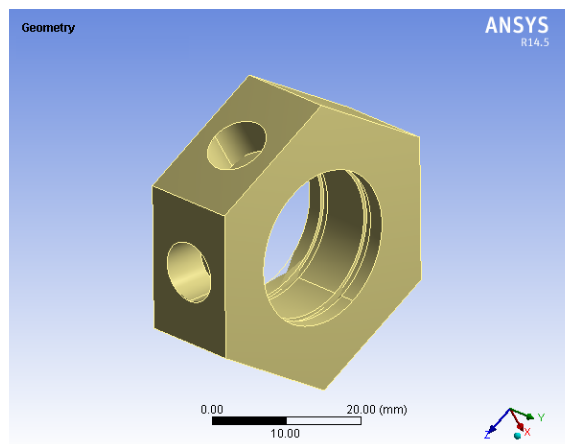

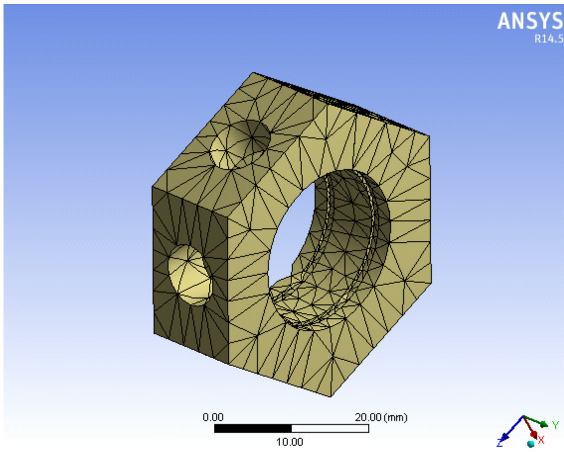

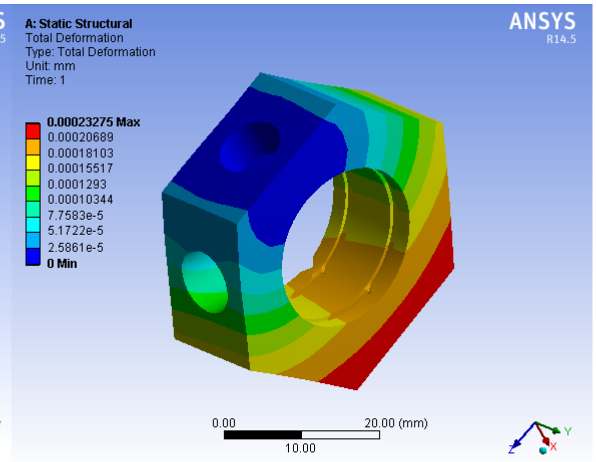

Fig 3.15.2: Ansys model of trunion holder

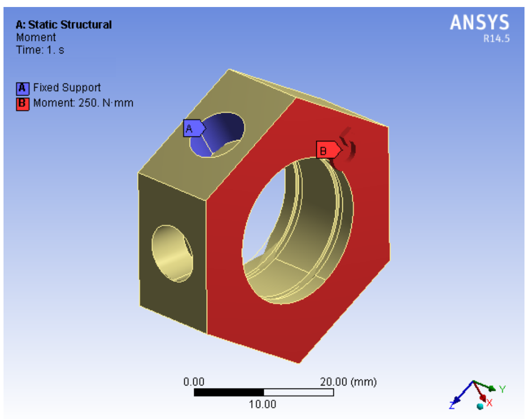

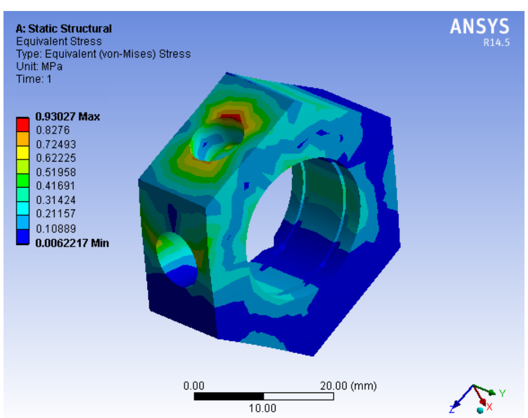

3.15.3 Result & Discussion

Part Name	Maximum theoretical stress N/mm^2	Von-mises stress N/mm^2	Total deformation mm	Result
Trunion holder	0.2	0.9	0.00023	Safe

Table3.15.3: Result table for trunion holder

3.15.4 Conclusion

a) Maximum stress by theoretical method and Von-mises stress are well below the allowable limit, hence the trunion holder is safe.

b) Trunion holder shows negligible deformation

4 EXPERIMENTAL VALIDATION

4.1Experimental Setup

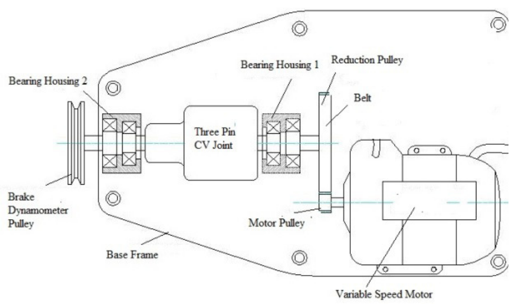

Figure4.1.1: setup for three pin constant velocity joint

4.2Test & Trial

4.2.1Coupling Bronze Trunion:

Parallel Offset: 12mm

Aim: To conduct trial and plot

a) Torque vs. Speed Characteristics

b) Power vs. Speed Characteristics

Arrangement: In order to conduct trial,a dynamobrake pulley cord, weight pan are provided on the output shaft.

Procedure:

a) Start motor.

b) Let mechanism run & stabilize at certain speed (say 1500 rpm).

c) Place the pulley cord on dynobrake pulley and add 0.1 Kg weight into, the pan, note down the output speed for this load by means of tachometer.

d) Add another 0.1 Kg cut & take reading.

e) Tabulate the readings in the observation table.

f) Plot Torque vs. speed characteristic.

g) Plot Power vs. speed characteristic..

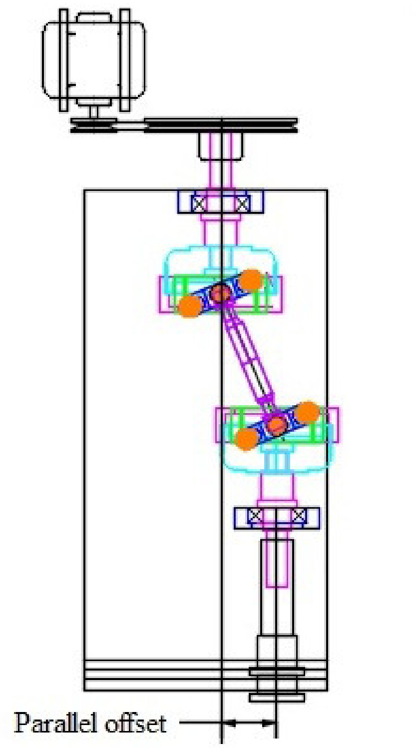

Fig 4.2.1: Experimental setup for parallel offset.

Observation Table

Sr. NO	Loading		Unloading		Mean speed
	Weight(KG)	Speed rpm	Weight (KG)	Speed rpm	
01	0.2	1480	2	1460	1470
02	0.4	1400	4	1410	1405
03	0.6	1320	6	1340	1330
04	0.8	1210	8	1190	1200
05	1.0	960	10	920	940

Table 4.2.1.1: Observation table for parallel offset

Sample Calculations:- (At .8 Kg Load)

Average speed :-

$$N = \frac{N_1 + N_2}{2} = \frac{1210 + 1190}{2} = 1200\text{rpm}$$

Output Torque:-

T_{dp} = Weight in pan x Radius of Dynobrake Pulley

= (0.8x 9.81) x 25

=196.2 N.mm

T_{dp}=0.1962 N.m

Input Power:- ($P_{i/p}$) = 29.6 Watt.

Output Power:-($P_{o/p}$)

$$P_{o/p} = \frac{2\,\Pi\, N T_{o/p}}{60}$$

$$= \frac{2 \times \Pi \times 0.1962 \times 1200}{60}$$

$P_{o/p}$ = 24.6 watt

Efficiency:-

$$\eta = \frac{\text{Output power}}{\text{Input power}}$$

$$= \frac{24.6}{29.6}$$

η = 83.10%

Efficiency of transmission of gear drive at 0.8 kg load= 83.10%

Result table

Sr. NO	Load (kg)	Speed (rpm)	Torque (N.M)	Power (watt)	Efficiency
	0.2	1470	0.04905	7.55164	25.5123
	0.4	1405	0.0981	14.43545	48.7684
	0.6	1330	0.14715	20.49731	69.24766
	0.8	1200	0.1962	24.65842	83.30546
	1.0	940	0.24525	24.1447	81.56993

Table 4.2.1.2: Result table for parallel offset

Characteristics Plots

Torque vs Speed

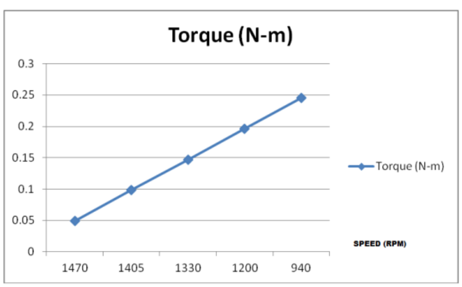

Graph shows that torque increases with decreasein output speed of coupling .

Power vs Speed

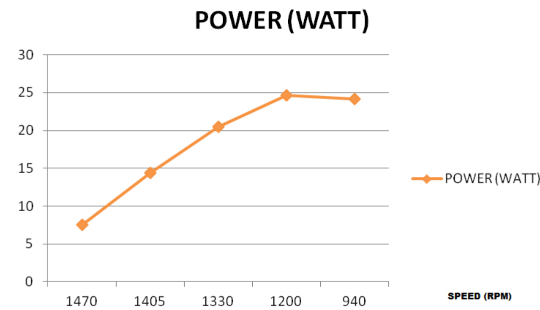

Graph shows that maximum power is delivered by the coupling at clos to 1200 rpm Thus this is recommended speed at maximum parallel offset condition.

Efficiency vs Speed

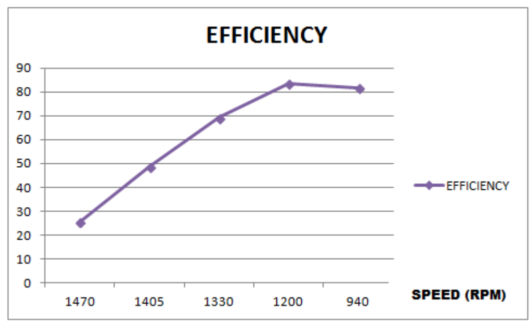

Graph shows that maximum efficiency is attained by the coupling at close to 1200 rpm Thus this is recommended speed at maximum parallel offset condition for maximum efficiency.

4.2.2EN-24 Trunion: Angular Offset: 14 Degree Maximum

Aim: To conduct trial and plot

a) Torque vs. Speed Characteristics
b) Power vs. Speed Characteristics

Arrangement: In order to conduct trial,a dynobrake pulley cord, weight pan are provided on the output shaft.

Procedure:

a) start motor
b) Let mechanism run & stabilize at certain speed (say 1500 rpm)
c) Place the pulley cord on dynmobrake pulley and add 0.1 Kg weight into, the pan, note down the output speed for this load by means of tachometer.
d) Add another 0.2 Kg cut & take reading.
e) Tabulate the readings in the observation table
f) Plot Torque vs. speed characteristic
g) Power vs. speed characteristic.

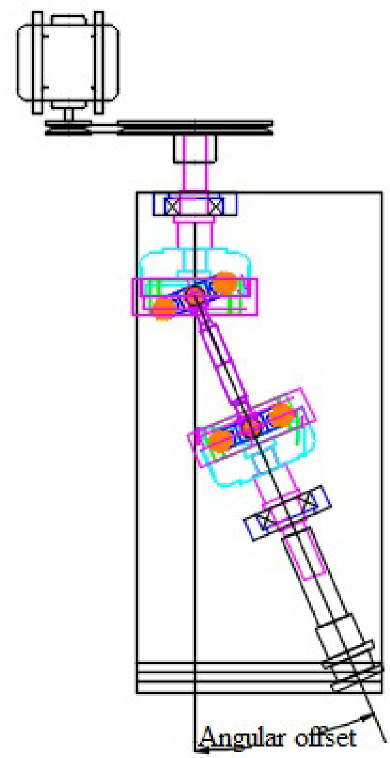

Fig 4.2.2: Experimental setup for angular offset.

Observation Table

Sr. NO	Loading		Unloding		Mean Speed
	Weight (Kg)	Speed rpm	Weight (Kg)	Speed rpm	
1	0.2	1440	2	1420	1430
2	0.4	1320	4	1310	1315
3	0.6	1220	6	1240	1230
4	0.8	1090	8	1080	1070
5	1.0	900	10	880	890

Table 4.2.2.1: observation table for angular offset

Result Table

Sr. NO	Load (kg)	Speed (rpm)	Torque (N.m)	Power (watt)	Efficiency (%)
	0.2	1430	0.04905	7.346153	24.81808
	0.4	1315	0.0981	13.51076	45.64445
	0.6	1230	0.14715	18.95616	64.04107
	0.8	1070	0.1962	21.98709	74.2807
	1.0	890	0.24525	22.86041	77.2311

Table 4.2.2.2: Result table for angular offset

Characteristics Plots

Torque vs Speed

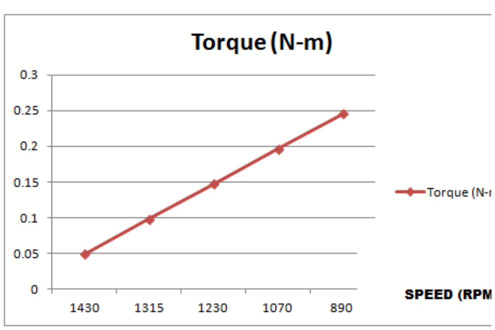

Graph shows that torque increases with decreasein output speed of coupling .

Power vs Speed

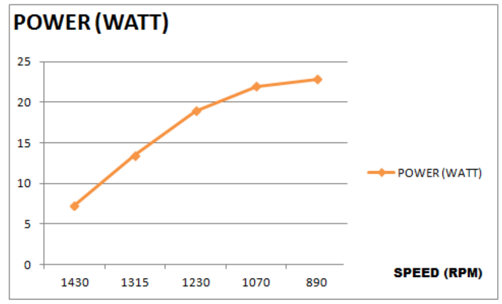

Graph shows that maximum power is delivered by the coupling at clos to 900 rpm .Thus this is recommended speed at maximum angular offset condition.

Efficiency vs Speed

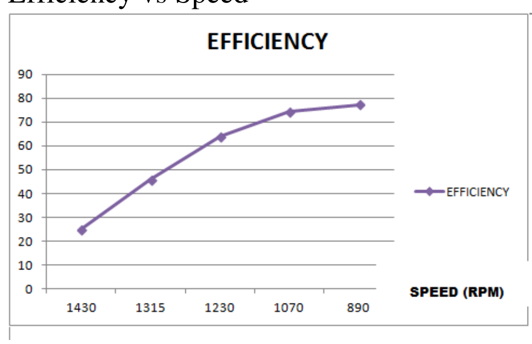

Graph shows that maximum efficiency is attained by the coupling at close to 900 rpm Thus this is recommended speed at maximum angular offset condition for mximum efficiency.

5 COST ANALYSIS

5.1 Bill of Materials

SR NO.	Part Code	Description	Quantity	Material
	TCVJ –1	Frame	01	MS
	TCVJ –2	Bearing Housing LPlate	02	EN9
	TCVJ –3	Bearing Housing	02	EN9
	TCVJ –4	Main Pulley	01	EN9
	TCVJ –5	Input Shaft	01	EN24
	TCVJ –6	Output Shaft	01	EN24
	TCVJ –7	Coupler Body	01	AL
	TCVJ –8	Coupling Female L	02	EN24
	TCVJ –9	Constrain Ring	02	EN24
.	TCVJ –10	Coupler Ring	02	EN24
.	TCVJ –11	Trunion Holder	02	AL
.	TCVJ –12	Trunion	03 EACH	BRASS/ BRONZE/EN24
.	TCVJ –13	Slide Bar	02	EN9
.	TCVJ –14	Slide Nut	02	EN9
.	TCVJ –15	Clamp Plate	01	EN9
.	TCVJ –16	Motor Plate	01	MS
.	TCVJ –17	Dyno Brake Pulley	01	CI
.	TCVJ –18	Bolt Rest	02	EN9
.	TCVJ –19	Motor	01	STD
.	TCVJ –20	Belt(6 X 600)	01	STD
.	TCVJ –21	Grub Screw M8 X 8	03	STD
.	TCVJ –22	Grub Screw M6 X 8	09	
.	TCVJ –23	HEX BOLT M8 X 25	02	
.	TCVJ –24	HEX BOLT M10 X 30	02	
.	TCVJ –25	Grub Screw M8 X 8	03	

Table 5.1: Material bills table

5.2 Raw Material Cost

The total raw material cost as per the individual materials and their corresponding ratesper kg is as follows,

Total raw material cost = Rs. 4150/-

5.3Machining Cost

Operation	Rate (Rs /Hr)	Total Time (Hrs)
Lathe	100	25
Milling	105	16
Jig Boring	90/Hole	9 No's
Drilling	50	4.2
Tapping	5 Rs/Hole	18
Slotting		
Total		

Table 6.3: Machining cost table

Total machining cost = Rs. 11990 /-

5.4 Miscellaneous Costs

Operation	Cost(Rs.)
Assembly	800
Fabrication	1280
Total	2080

Table 5.4: Miscellaneous cost table

5.5 Cost of Purchased Parts

Sr No.	Description	Quantity	Cost
	Motor	01	1150
	Srdg Brg 6004zz	02	500
	Dyno Brake Pulley	01	210
	Belt	01	170
	Circlips	09	130
	Grub Screw M8	03	12
	Grub Screw M6	9	27
	Bolts & Nut	-	166

Table 5.5: Table of costs of purchased parts

The cost of purchase parts = Rs 2365/-

5.6 Total Cost

Total cost = Raw Material Cost +Machine Cost + Miscellaneous Cost + Cost of Purchased Parts +Overheads

Hence the total cost of machine = Rs 13600/-/-approx.

7 SCOPE FOR FUTURE WORK

a) It is replacement to all present velocity joints.

b) One can reduce the cost and space required so that it will easily penetrate in the market.

c) Its efficiency can be increased up to 95% by using antifriction material.

d) If there are any hely design, that could apply this mechanism.

e) It is remarkable device to be used in industries, plane, helicopters, trains, tractors etc.

8 CONCUSION

Three pin constant velocity joint is replacement to all present velocity joint.One can reduce the cost and space required so that it will easily penetrate in the market.Its efficiency can be increased up to 95% with antifriction material. It has less vibrations and less friction, hence runs cool. It is remarkable device to be used in industries, plane, helicopters, trains, tractors etc. From this project stage 1 on three pin constant velocity joint we will be able to conclude that it is a joint with higher parallel and angular misalignment capability and it can be preferred over universal joint.

Thus we have performed analysis on 3 pin constant velocity joint for parallel and angular power transmission. We have conducted trial on 3 pin constant velocity joint
andrecorded the readings. We have plotted performance characteristics of the joint such as torque vs speed, power vs speed and efficiency vs speed both for parallel and angular power transmission. From the trial we can conclude that the joint has better performance characteristics than universal joint.

9REFERENCES

a) "Design of machine elements", V. B. Bhandari, the McGraw-Hill Companies,2nd edition, 2009.

b) "Machine Design Data Book", V. B. Bhandari; McGraw-Hill Publication August 2014.

c) "A Textbook of Theory of Machines", Dr. R. K. Bansal, Dr. J. S. Brar, Laxmi Publications (P) LTD, 5th edition, October 2011.

d) Ian Watson, B. Gangadhara Prusty, John Olsen. Conceptual design optimization of a constant velocity coupling. Mechanism and Machine Theory 68 (2013), Page No. 18–34.

e) Chul-Hee Lee, Andreas A. Polycarpou. A phenomenological friction model of tripod constant velocity (CV) joints. Tribology International 43 (2010) Page No. 844–858.

f) Majid Yaghoubi, Seyed Saeid Mohtasebi, Ali Jafary, Hamid Khaleghi. Design, manufacture and evaluation of a new and simple mechanism for transmission of power between intersecting shafts up to 135 degrees (Persian Joint). Mechanism and Machine Theory 46 (2011) Page No. 861-868.

g) Katsumi Watanabe, Takashi Matsuura. Kinematic Analyses of Rzeppa Constant Velocity Joint by Means of Bilaterally Symmetrical Circular-Arc-Bar Joint.

h) Tae-Wan Ku, Lee-Ho Kim, Beom-Soo Kang. Multi-stage cold forging and experimental investigation for the outer race of constant velocity joints. Materials and Design 49 (2013) Page No. 368–385.